jet INTL JOURNAL OF ELECTRONICS AND TELECOMMUNICATIONS, 2011, VOL. 57, NO. 4, PP. 503–509
Manuscript received October 17, 2011; revised November 2011. DOI: 10.2478/v10177-011-0071-2

A Simplified Design Methodology for MOSFET-Only Wideband Mixer

Eduardo Ortigueira, Ivan Bastos, Luís B. Oliveira, João P. Oliveira, and João Goes

***Abstract*—In this paper we present a MOSFET-only implementation of a wideband Gilbert Cell. The circuit uses a common-gate topology for a wideband input match, capable to cover the Wireless Medical Telemetry Service (WMTS) frequency bands of 600 MHz and 1.4 GHz. In this circuit the load resistors are replaced by transistors in triode region, to reduce area and cost, and minimize the effects of process and supply variations and mismatches. In addition, we obtain a higher gain for the same DC voltage drop, with a reduced impact on the noise figure (NF). The performance of this topology is compared with that of a conventional mixer with load resistors. Simulation results show that a peak gain of 20.6 dB (about 6 dB improvement) and a NF about of 11 dB for the 600 MHz band. The total power consumption is 3.6 mW from a 1.2 V supply.**

***Keywords*—CMOS mixers, MOSFET-only circuits, Gilbert cell, active mixers, wideband mixers.**

I. Introduction

NOWADAYS, the demand for mobile and portable equipment has led to a large increase in wireless communication applications. In order to achieve full integration and low cost modern receiver architectures (Low-IF and Zero-IF receivers), inductorless circuits are required [1]–[5].

In modern communication systems the mixer plays a vital part, either used in reception or transmission [6]–[8]. It requires a careful design specially when used in receivers, since generally in a receiver the input signal is a low power signal. Therefore, the mixer should be able to ensure enough conversion gain to relax the performance requirements of both: previous and following blocks (using active devices). Adding this factor they are also commonly implemented in CMOS technology since it reduces cost, enables high integration and high frequency performance.

In this work an active mixer is presented, based on the Gilbert Cell. Its behavior and performance will be examined according to a qualitative and straightforward design methodology, and it will be shown that even though distortion generation mechanisms are not taken in account the approximations used to determine the gain and NF are accurate.

Inductorless circuits have reduced die area and cost [4]. However, they are usually realized with MiM capacitors, which require an additional insulator/metal layer, and they use poly or/and diffusion resistors, which have large process variations and mismatches [9].

In this paper our main goal is to design a high gain, very low area and low-cost wideband mixer, and at the same time obtain less circuit variability, by implementing the resistors using MOS transistors (MOSFET-only design) [10]. As it will be shown, this approach adds a new degree of freedom, which can be used to maximize the mixer gain, with a minimum impact in the circuit NF.

For the complete mixer we compare the conventional design with resistors, and the new MOSFET-only implementation in terms of gain and NF. Simulation results of a circuit example designed in a standard 130 nm CMOS technology validate the proposed methodology.

The circuit presented in this paper is intended for use in the WMTS, which establishes wireless communication between an externally worn medical device and other equipment [5]. There are three frequency bands allocated to WMTS: 608 – 614 MHz, 1395 – 1400 MHz and 1427 – 1432 MHz. With the proposed circuit we intend to cover all the bands allowed for these applications.

II. MOSFET-Only Cell Mixer

A. Current Commutating Mixer Basics

It is well known that depending on the amplitude of input signal, the differential pair of Fig. 1 can act as a current commutating stage, which enables the implementation of a simple mixing operation, [6]. The conversion from current to a voltage signal at the output can be achieved by a resistor load, R_D, which has to be considered for both: conversion gain and noise performance. An alternative approach is to replace these pure resistive loads by active ones, based on PMOS devices, which are usually sized for saturation. This has the advantage of improving the overall gain, but the output DC common mode level might have to be adjusted by means of additional circuitry, without affecting distortion (IIP3 and IIP2). Instead, this work explores the use of active loads operating in triode region, which simplifies the overall process design, minimizing the distortion penalty.

The switching operation of the differential circuit represented in Fig. 1 is obtained when a large signal (e.g., coming from a local oscillator, v_{LO} is applied at the gates of the differential pair. To act as an active mixer (meaning an effective conversion gain), M_1 and M_2 are preferably switched between saturation and OFF states. Not only the switching function is guaranteed, but also, when saturated, the transistor acts as a current buffer relatively to the current signal injected

This work was supported by the Portuguese Foundation for Science and Technology and CTS-UNINOVA multiannual funding through the PIDDAC program funds.

E. Ortigueira, I. Bastos, L. B. Oliveira, J. P. Oliveira, and J. Goes are with CTS-UNINOVA, Departamento de Engenharia Electrotécnica, Faculdade de Ciências e Tecnologia, FCT, Universidade Nova de Lisboa, Monte da Caparica, Portugal (e-mail: l.oliveira@fct.unl.pt).

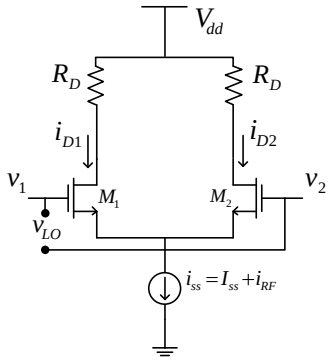

Fig. 1. CMOS differential pair.

at the source terminal. Under these conditions, their bias point can be considered to vary periodically in time, [6], and the current flowing in each branch depends not only on the biasing current, I_{SS}, but also on the differential voltage v_{LO}, as it is demonstrated by

$$i_{D1} = \frac{I_{SS}}{2} + \frac{I_{SS}}{2}\frac{v_{LO}}{(V_{gs}-V_t)^2}\sqrt{1-\frac{1}{4}\left(\frac{v_{LO}}{V_{gs}-V_t}\right)^2}$$
$$i_{D2} = \frac{I_{SS}}{2} - \frac{I_{SS}}{2}\frac{v_{LO}}{(V_{gs}-V_t)^2}\sqrt{1-\frac{1}{4}\left(\frac{v_{LO}}{V_{gs}-V_t}\right)^2}, \quad (1)$$

where the transistors where assumed to be saturated (when conducting) and V_t is the threshold voltage. These results clearly show that when the differential voltage v_{LO} is greater than V_{dsat} (given by $V_{gs}-V_t$) one of the transistors switches off and the current flows only through one branch. When the instantaneous local oscillator (LO) differential voltage v_{LO} is lower than V_{dsat}, the biasing current is then balanced between the two branches. During this last interval, the differential pair presents a higher transconductance increasing the noise contribution at the output.

The analysis of the circuit presented relies mostly on the common differential pair analysis. In a common differential pair, the parameters can be easily retrieved considering a linear behavior where it is assumed that we are facing weakly variations. However, the same approach can be done when the differential pair is working over the non-linear region of its I-V characteristic. If we consider that the differential pair has a periodic behavior thus having also periodic parameters, a time evaluation of the circuit behavior will allow to achieve average parameters value. This means the circuit characterization can be made as similar as the one done over the linear region but with average values.

B. Conversion Gain

The previous circuit can be used as a single balanced mixer, if we superimpose the incoming RF signal on the bias current source, i_{SS}. Then the mixing effect is obtained through current commutation (mixing is done in the current domain), since the variable current will be translated to the output of the mixer at the switching frequency, which results in a frequency translation of the input signal. A key parameter of the mixer is the achievable conversion gain, which measures the relation between the signal strength at the IF and the RF incoming signal. A new circuit technique to maximize this gain is the main goal of this paper. If a periodic v_{LO} is used with amplitude high enough, the time that both transistors are active is reduced significantly. It is important to clarify that both transistors in the dynamic regime should alternate between the saturation region and cut-off, to achieve a conversion gain higher than one. By taking into account the previously determined current equations, one can define a function which relates the output current as a function of the instantaneous LO voltage $v_{LO}(t)$ and the input current, [6], [7],

$$I_0 + i_0 = i_{D1} - i_{D2} = F\left(v_{LO}\left(t\right), i_{SS}\right), \quad (2)$$

where I_0 and i_0 are the differential output mixer currents.

For a periodic local oscillator, then it can be assumed that the differential pair has a periodically time-varying behavior, which a first order response can be obtained by taking the firsts components of the Taylor expansion:

$$I_0 = F\left(v_{LO}(t), i_{SS}\right) = p_0(t)$$
$$i_0 = \frac{\delta F(v_{LO}\left(t\right), i_{SS})}{\delta I_{SS}} i_{RF} = p_1(t) i_{RF}, \quad (3)$$

where $p_1(t)$ represents the periodic trapezoidal function caused by the LO, which is shown in Fig. 2.

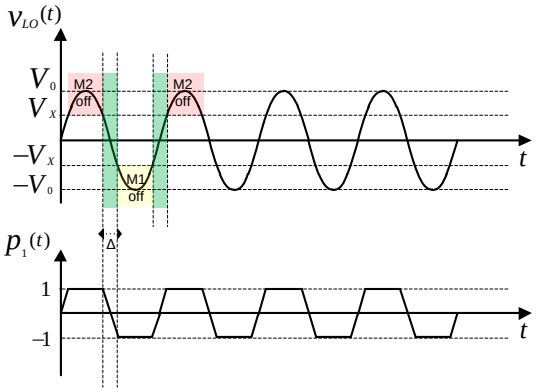

Fig. 2. Switching pair first order response, according to [6], [7].

As one can see, using a sine-wave to drive the switching pair, instantaneous switching is not possible and the current output instead of a perfect square wave will resemble a trapezoid wave. Thus, to determine the conversion mixing gain, it is important to expand the periodic wave $p_1(t)$, by means of a Fourier analysis. For simplicity, it is considered that over the time window Δ (see Fig. 2), the current varies linearly with time. The trapezoidal signal can be obtained by subtracting a triangular signal, Fig. 3(a), to the square wave signal. Therefore, they will be analyzed separately. The Fourier coefficients of a square wave are given by,

$$R_n = \frac{1}{T_{LO}} \int_{-\frac{T_{LO}}{2}}^{-\frac{T_{LO}}{2}} rect\,(t)\, e^{-\frac{j2\pi n}{T_{LO}} t}\, dt = \frac{-2j}{T_{LO}} \int_{0}^{-\frac{T_{LO}}{2}} \sin\left(\frac{2\pi n}{T_{LO}} t\right) dt = \frac{j}{\pi n}\left[(-1)^n - 1\right] \tag{4}$$

For the coefficients of the triangular wave, we need to firstly describe an auxiliary function $f(t)$, represented in Fig. 3(b) and it is described by

$$f\,(t) = \frac{2}{\Delta} t + 1 \tag{5}$$

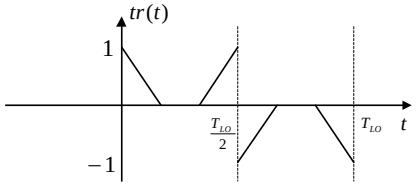

(a)

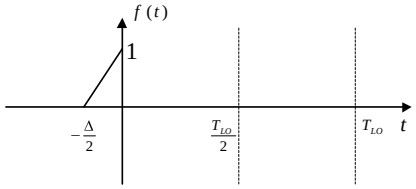

(b)

Fig. 3. a) Triangular wave, b) auxiliary function $f(t)$.

The respective Fourier coefficients are then obtained by,

$$F_n = \frac{1}{T_{LO}} \int_{-\frac{\Delta}{2}}^{0} f\,(t)\, e^{-\frac{j2\pi n}{T_{LO}} t}\, dt = \frac{1}{T_{LO}} \int_{-\frac{\Delta}{2}}^{0} \left(\frac{2}{\Delta} t + 1\right) e^{-\frac{j2\pi n}{T_{LO}} t}\, dt = -\frac{1}{j2\pi n} + \frac{2T_{LO}}{\Delta\,(2\pi n)^2}\left(1 - e^{\frac{j\Delta\pi}{T_{LO}} n}\right), \tag{6}$$

resulting on the triangular wave coefficients given by,

$$\begin{aligned} Tr_n &= F_{-n} + F_n.e^{-\frac{j2\pi n}{T_{LO}}\frac{T_{LO}}{2}} - F_{-n}.e^{-\frac{j2\pi n}{T_{LO}}\frac{T_{LO}}{2}} - F_n.e^{-\frac{j2\pi n}{T_{LO}} T_{LO}} \\ &= F_{-n} + (-1)^n\,(F_n - F_{-n}) - F_n \\ &= ((-1)^n - 1)\,(F_n - F_{-n}) \\ &= ((-1)^n - 1)\left[-\frac{1}{j\pi n} + \frac{2T_{LO}}{\Delta\,(2\pi n)^2}\left(-e^{\frac{j\Delta\pi}{T_{LO}} n} + e^{-\frac{j\Delta\pi}{T_{LO}} n}\right)\right] \end{aligned} \tag{7}$$

Using Euler's trigonometric relation,

$$Tr_n = ((-1)^n - 1)\left[-\frac{1}{j\pi n} + \frac{2T_{LO}}{\Delta\,(2\pi n)^2} 2j \sin\left(\frac{\Delta\pi}{T_{LO}} n\right)\right] = [(-1)^n - 1]\left[-\frac{1}{j\pi n} + \frac{jT_{LO}}{\Delta\,(\pi n)^2} \sin\left(\frac{\Delta\pi}{T_{LO}} n\right)\right] \tag{8}$$

one can obtain the periodic waveform $p_1(t)$ coefficients, resulting in,

$$\begin{aligned} P_{1_n} &= R_n - TR_n \\ P_{1_n} &= [(-1)^n - 1]\left[\frac{j}{\pi n} + \frac{1}{j\pi n} - \frac{jT_{LO}}{\Delta\,(\pi n)^2} \sin\left(\frac{\Delta\pi}{T_{LO}} n\right)\right]. \end{aligned} \tag{9}$$

The previous analysis takes into account half of the coefficients. For a full characterization, from the Fourier expansion for a generic function $x(t)$,

$$\sum_{-\infty}^{\infty} X_n e^{\frac{j2\pi}{T} nt} = 2j \sum_{1}^{\infty} |X_n| \sin\left(\frac{2\pi}{T} nt\right) \tag{10}$$

and considering only the odd order coefficients (even order are canceled due to the differential structure of the mixer) the periodic wave $p_1(t)$ is finally given by

$$p_1\,(t) = \sum_{1}^{\infty} \left| \frac{4}{\pi(2n-1)} sinc\left(\frac{\Delta\pi}{T_{LO}}(2n-1)\right) \right| \sin\left(\frac{2\pi}{T_{LO}}(2n-1)t\right). \tag{11}$$

Considering a differential structure and only the first harmonic, one can obtain for the output differential current

$$i_0 = \frac{4}{\pi} sinc(\Delta\pi f_{LO}) \sin\left(\omega_{LO} t\right) i_{RF}\,(t)\,, \tag{12}$$

where

$$\pi\Delta f_{LO} = \arcsin\left(\frac{V_x}{V_{LO}}\right). \tag{13}$$

In a practical mixer implementation there is no instantaneous switching, which leads to power loss at the band of interest. This loss is linked with the slope of the current characteristic during the time window Δ. But if we consider a high value of LO amplitude ($\Delta << T_{LO}$), the characteristic is almost ideal, meaning that,

$$i_0 = \frac{4}{\pi} \sin\left(\omega_{LO} t\right) i_{RF}\,(t) \tag{14}$$

If the transconductance stage is implemented as a common gate (CG) topology, shown in Fig. 4, with $g_{ds_{CG}} << g_{m_{SW}}$, then the current i_{RF} is given by,

$$i_{RF} = (g_{m_{CG}} + g_{mb_{CG}}).v_{in}\,(\omega_{RF} t) \tag{15}$$

where the transistor bulk transconductance, $g_{mb_{CG}}$, has been included.

Finally, the total mixer transconductance conversion gain is then given by

$$g_c = \frac{i_0\,(\omega_{IF} t)}{v_{in}\,(\omega_{RF} t)} = \frac{2}{\pi}(g_{m_{CG}} + g_{mb_{CG}}). \tag{16}$$

C. Mixer Voltage Conversion Gain

Since the main objective of this work is to implement a low area wideband mixer, instead of using load resistors, MOS transistors operating in triode region are employed. The main idea is that, a higher equivalent resistance can be achieved for the same DC voltages drop, when compared to a resistive load. Moreover, this approach aims to minimize the effects of process and supply variations and mismatches, [9], [10]. For simplicity, it will be considered that the equivalent load impedance is just given by $\frac{1}{g_{ds,D}}$ (as seen in Fig. 4). Then the AC voltage conversion gain can be simply determined since

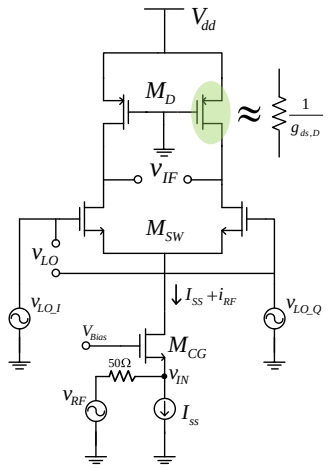

Fig. 4. CMOS differential pair with active loads.

the switching pair can be seen as an amplifier with linear gain equal to $\frac{2}{\pi}$ with source degeneration impedance, and resistive load:

$$A_c = \frac{2}{\pi}\frac{1}{g_{ds,D}}\frac{1}{Z_e}, \text{with } Z_e \approx (g_{m_{CG}} + g_{mb_{CG}}) << g_{ds,D}$$
$$A_c \approx \frac{2}{\pi}\frac{(g_{m_{CG}} + g_{mb_{CG}})}{g_{ds,D}} \tag{17}$$

where it is assumed that the output conductance of the switching pair is much greater than the load impedance (these transistor pair operating in saturation acts as current buffer).

D. Noise Analysis

To analyze the noise produced by the MOSFET-only mixer, one should determine the amount of time, Δ, in which the switching pair is acting as a gain block, as shown in Fig. 5.

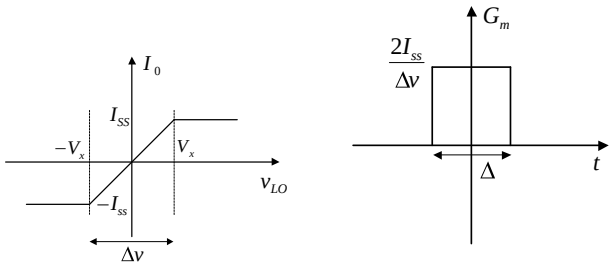

Fig. 5. a) Switching pair I-V relation, b) transconductance during Δ.

$$G_m(t) = 2\frac{g_{m1}(t)g_{m2}(t)}{g_{m1}(t) + g_{m2}(t)} \tag{18}$$

During the time window Δ, when both transistors are conducting and the output is defined according a current division, the output current has a linear (a rough approximation)

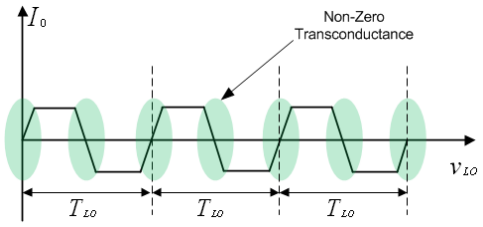

Fig. 6. Non-zero transconductance.

dependency on the voltage v_{LO}, which produces a non-zero transconductance.

At this point it is important to clarify that it was assumed that the differential pair should alternate between saturation and cut off to achieve conversion gain. This is merely because even though a similar time response (see Fig. 6) could be achieved if the transitions between triode and cut off were done (thus allowing the same transconductance description), the resulting output impedance of the circuit would be mainly dependent on the AC equivalent of a transistor operating in triode region, that as we know is approximated by a low impedance resistance. This means that, the circuit performance would be dependent on the output conductance of the differential pair instead of the load impedance. Since this transconductance it is not defined over the entire period of the oscillator, it is important to determine its average value during T_{LO}, taking also into account that this transconductance is defined twice per period (as seen in Fig. 6)

$$\overline{G}_m = \frac{2}{T_{LO}}\int_0^{\frac{T_{LO}}{2}} G_m(t)\, dt. \tag{19}$$

By changing the variable of integration from t to v_{LO},

$$\overline{G}_m = \frac{2}{\pi V_{LO}}\int_{-V_x}^{V_x} G_m(v_{LO})\frac{1}{\sqrt{1-\left(\frac{v_{LO}}{V_{LO}}\right)^2}}\, dv_{LO}. \tag{20}$$

Since v_{LO} in the interval is much smaller than V_{LO} the average value of the periodic transconductance is then given by [6]–[8]:

$$\overline{G}_m = \frac{4}{\pi V_{LO}}\int_{-V_x}^{V_x}\frac{\delta I_0}{\delta v_{LO}}\, dv_{LO} = \frac{4}{\pi}\frac{I_{SS}}{V_{LO}}. \tag{21}$$

To analyze the mixer noise, we will consider first the thermal noise of the switching pair. This is a common source stage (perfect match allows bisection theorem appliance), but instead of using a transconductance value obtained from a static operation point, it will be used the average transconductance (21), [9]. Then the input CG thermal noise, which appears at the output will be determined taking into account the level of mismatch at the input, the aliasing effects associated with the oscillator harmonics (several harmonics will translate RF transconductance white noise to the IF output), and the conversion gain. The thermal noise generated by the switching pair is given by

$$\overline{V_{o\,n_{th},sw}^2} = 4kT\gamma\overline{G}_m\left(\frac{1}{g_{ds,D}}\right)^2 = 4kT\gamma\frac{4}{\pi}\frac{I_{SS}}{V_{LO}}\left(\frac{1}{g_{ds,D}}\right)^2. \tag{22}$$

The thermal noise generated by the CG can be calculated from,

$$\begin{aligned}\overline{V_{o\,n_{th},cg}^2} &= N\overline{V_{n_{th},CG}^2}(A_c\alpha)^2 \\ \alpha &= \frac{1}{[1+(g_{m_{CG}}+g_{mb_{CG}})R_S]},\end{aligned} \tag{23}$$

where N represents the power accumulated from all the oscillator harmonics aliasing effects, which can be determined applying the Parseval's identity

$$P = \frac{1}{T_{LO}}\int_{-\frac{T_{LO}}{2}}^{-\frac{T_{LO}}{2}} |rect\,(t)\,|^2\,dt = \sum_{-\infty}^{\infty}|R_n|^2 = \sum_{1}^{\infty}\frac{8}{\pi^2(2n-1)^2}. \tag{24}$$

Then, the CG thermal noise present at the output is just given by

$$\overline{V_{o\,n_{th},cg}^2} = 2kT\gamma(g_{m_{CG}}+g_{mb_{CG}})\left[\frac{1}{g_{ds,D}[1+(g_{m_{CG}}+g_{mb_{CG}})R_S]}\right]^2 \tag{25}$$

Finally, the thermal noises generated by the source and load resistances is

$$\begin{aligned}\overline{V_{o\,n_{th},R_S}^2} &= N\overline{V_{n_{th},R_S}^2}(A_c\alpha)^2 \\ &= 2kTR_S\left[\frac{g_{m_{CG}}+g_{mb_{CG}}}{g_{ds,D}[1+(g_{m_{CG}}+g_{mb_{CG}})R_S]}\right]^2. \\ \overline{V_{o\,n_{th},R_D}^2} &= \frac{8kT}{g_{ds,D}}.\end{aligned} \tag{26}$$

Defined all the noise sources, the total noise at the output is given by,

$$\overline{V_{o\,n,mixer}^2} = \overline{V_{o\,n_{th},R_S}^2} + \overline{V_{o\,n_{th},sw}^2} + \overline{V_{o\,n_{th},cg}^2} + \overline{V_{o\,n_{th},R_D}^2} \tag{27}$$

from which the single-sideband (SSB) NF can be determined by

$$NF = \frac{\overline{V_{o\,n,mixer}^2}}{\overline{V^2}_{n_{th},R_S}(A_c\alpha)^2} = \frac{\overline{V_{o\,n,mixer}^2}}{\overline{V_{o\,n_{th},R_S}^2}}. \tag{28}$$

The previous considerations results in the following approximation for the total mixer noise figure:

$$\begin{aligned}NF = 1 + \frac{1}{R_S(g_{m_{CG}}+g_{mb_{CG}})^2}\left[\left(\gamma\frac{8}{\pi}\frac{I_{SS}}{V_{LO}}+4g_{ds,d}\right)\right. \\ \left.[1+(g_{m_{CG}}+g_{mb_{CG}})R_S]^2+\gamma(g_{m_{CG}}+g_{mb_{CG}})\right].\end{aligned} \tag{29}$$

The Gilbert Cell, shown in Fig. 7, is based on two single balanced mixers and, therefore, both conversion gain and NF can be extrapolated from the previous results (30,31). A closer analysis of the circuit reveals that each single balanced mixer does not produce the highest output at the same time, so the differential factor of two is not applicable. Hence, the conversion gain of the Gilbert Cell is equal to the one of the single balanced mixer, as indication in equation (17) [6]–[8]. As far it concerns the noise, apart from the contribution of the load impedance, the noise is twice the single balanced mixer noise.

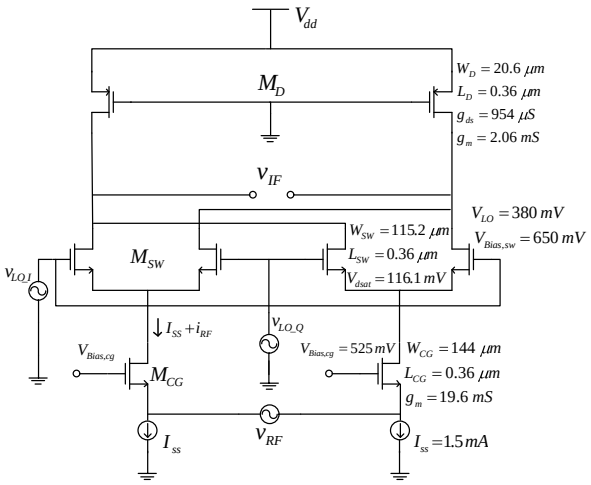

Fig. 7. Wideband Gilbert Cell.

$$A_c = 20\log\left[\frac{2}{\pi}\frac{(g_{m_{CG}}+g_{mb_{CG}})}{g_{ds,D}}\right] \tag{30}$$

$$\begin{aligned}NF = 10\log\left[1+\frac{2}{R_S(g_{m_{CG}}+g_{mb_{CG}})^2}\left[\left(\gamma\frac{8}{\pi}\frac{I_{SS}}{V_{LO}}+2g_{ds,d}\right)\right.\right. \\ \left.\left.[1+(g_{m_{CG}}+g_{mb_{CG}})R_S]^2+\gamma(g_{m_{CG}}+g_{mb_{CG}})\right]\right].\end{aligned} \tag{31}$$

E. Proposed Design Methodology

The design follows a transistor sizing approach that begins with the RF transconductance stage, continues by sizing the mixing stage, and finally the active load is sized. When compared with a pure resistive load, the PMOS active loads in triode region can reach higher load AC resistance for the same DC biasing, thus improving conversion gain and facilitating output voltage swing. The complete process involves:

1) Firstly, a low current source is selected in order to understate the power consumption;
2) From the previous current, the CG RF transistor is sized in order to reach a transconductance level compatible with a 50 Ω input impedance matching. The transistor gate biasing voltage is chosen so that the transistor is kept always in saturation region.
3) Afterwards, the transistors of the switching pairs, which perform the mixing operation, are sized in order to be in saturation during the ON cycle while maintaining non-conducting state during OFF cycle. Their sizes also have to ensure a low impedance node between the RF and mixing stage while at the output IF node their output resistance shall be much higher than the active loads. In other words, $g_{ds,sw} << g_{ds,D}$, and $\frac{g_{m,sw}}{2} << g_{ds,CG}$;
4) To ensure that a strong and well defined switching operation at the mixing stage, the V_{LO} is selected to be larger than $\sqrt{2}V_{dsat}$. However, additional headroom has to be taken into account to accommodate second order parasitic effects.

5) Finally the PMOS active loads are sized. The optimization is reached, by putting them in triode region, but sufficiently close to saturation (to improve small signal resistance). The final widths are then fine tuned in order to obtain sharper switching current transitions.

III. Simulation Results

To validate the theoretical equations, first the circuit is simulated with resistors (the resistance value is selected in order to maintain the same DC point) with a value of 433 Ω. The simulations were made with Cadence Spectre RF using BSIM3v3 for a 130 nm MOS technology. RF frequencies of 600 MHz and 1400 MHz were considered. The amplitude of the RF input signal is set to 2 mV. This circuit has a power consumption of only 3.6 mW drawn from a 1.2 V power supply. Under these design values, a theoretical voltage conversion gain of 14.65 dB, and a noise factor of 9.1 dB are estimated.

TABLE I
Gilbert Cell Conversion Gain and Noise Factor Using Resistive Loads

	Gilbert Cell w/ res.			
	600 MHz		1400 MHz	
$IF(MHz)$	$A_c(dB)$	$NF(dB)$	$A_c(dB)$	$NF(dB)$
20	14.27	9.6	12.5	10.4
40	14.25	9.6	12.5	10.4
60	14.16	9.6	12.5	10.4
80	14.16	9.6	12.5	10.3
100	14.07	9.6	12.5	10.3

The simulations results in Tab. I show that the approximations used results on a maximum error of 15 % for the conversion gain and a maximum error of 12.5 % for NF over the WMTS band. The results show a degradation as the frequency is increased, which is an expected result due to the parasitic effects.

Afterwards the circuit is simulated with the active loads in triode region. A MOS transistor operating in triode region can be modeled by a resistor only if $\frac{g_{ds}}{g_m} > 10$ (the saturation region is reached when g_m is of about the same magnitude as g_{ds}), otherwise the transistor should be modeled by a resistance in parallel with a current source. In this case we can increase the incremental load resistance without increasing the DC voltage drop. This allows the gain to be increased with respect to the circuit with "true" resistors. A theoretical conversion gain of 22.3 dB, and a noise factor of 8.4 dB are estimated. The simulation results show a maximum conversion gain of 20.3 dB and a maximum NF of 10.5 dB as seen in Fig. 8.

As shown in Fig. 9, in order to maintain the transconductance and switching stages under saturation, the size of the triode load has a limited range (as it enters in region A the output impedance becomes so large that the saturation, is not achievable in all transistors and the gain begins to collapse). Maximizing gain, means to choose a load transistor width close to the optimal point, shown in Fig. 9.

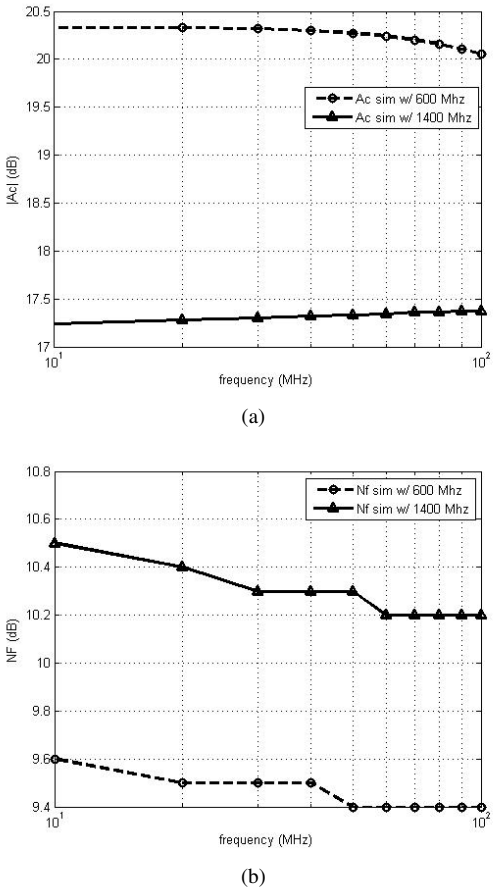

Fig. 8. (a Conversion gain (A_c) curve, b) Noise factor (NF) curve.

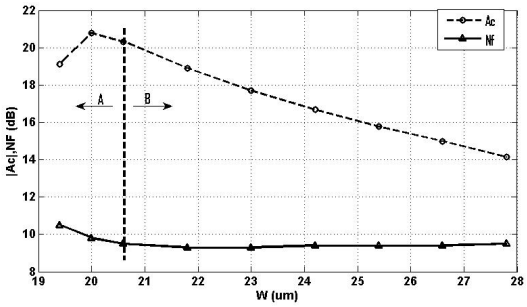

Fig. 9. Conversion gain (A_c) and noise (NF) for a variable transistor width.

TABLE II
Active Load versus Resistive Load over the 600 MHz Band

	G. Cell w/ MOS. (1048 Ω)		G. Cell w/ Res. (433 Ω)	
$IF(Mhz)$	$A_c(dB)$	$NF(dB)$	$A_c(dB)$	$NF(dB)$
20	20.33	9.5	14.27	9.6
100	20.05	9.4	14.07	9.6

In Tab. II a comparison is made between the simulated results obtained for the mixer when using pure resistive load and alternative triode ones. The DC voltage drops between the two cases are maintained. As expected, an improvement of the conversion gain is obtained with similar NF level. The effect of the flicker noise is reduced since the used IF frequency is sufficiently away from the $\frac{1}{f}$ corner frequency. Finally, the

IIP3 of both implementations is simulated for comparison (see Fig. 10(a) and Fig. 10(b)). The implementation with resistors presented an IIP3 value of –6.06 dBm and a IIP3 value of –8.22 dBm for the implementation with active loads. As we can conclude the use of load in triode region does not have significant impact of the mixer linearity.

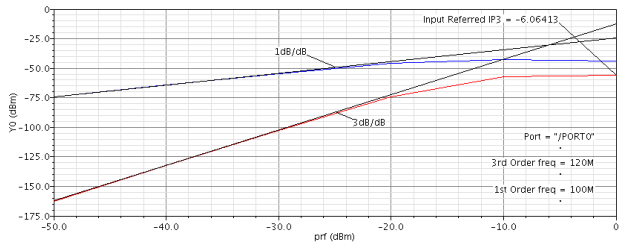

(a)

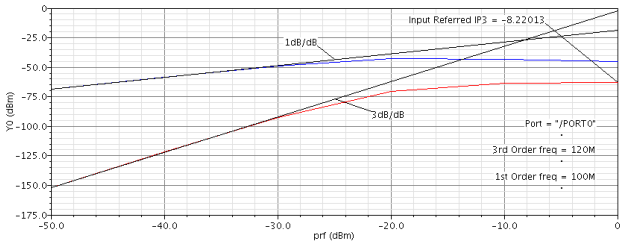

(b)

Fig. 10. a) Gilbert Cell IIP3 with resistors, b) Gilbert Cell IIP3 with active loads.

If we consider the optimal design point, where the Signal to Noise ratio is improved, we can see that the switching pair current commutation characteristic is not well behaved as shown in Fig. 11, and yet good performance and accurate approximations were achieved.

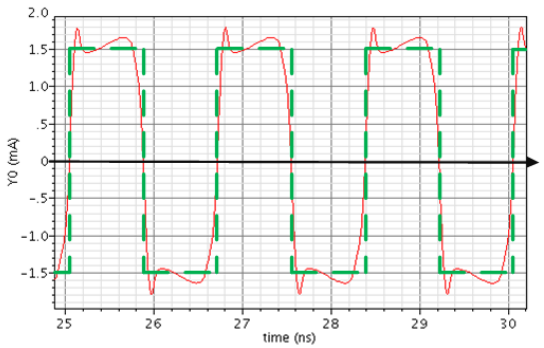

Fig. 11. Switching pair current characteristic in the optimal point as seen in Fig. 9.

By hypothesis, if we relax the current characteristic (meaning that the current gain is no longer $\frac{2}{\pi}$, due to slower transitions) and at the same time ensure that,

$$\frac{2}{\pi} sinc(\Delta\pi f_{LO})(g_{m_{CG}} + g_{mb_{CG}}) << \frac{1}{g_{ds,D}} \quad (32)$$

the circuit is likely to be optimized without affecting significantly both conversion gain and NF. Under those conditions, comparable performance can be obtained with reduction of the LO power and/or reduction of the switching pair width.

IV. Conclusion

In this paper we presented a MOSFET-only implementation of a Gilbert Cell, based in a CG wideband input match. In MOSFET-only circuits, the replacement of resistors by transistors reduces the area and cost and minimizes the effect of process and supply variation and of mismatches. The new approach proposed here adds a new degree of freedom, which can be used to optimize the mixer gain: we can obtain a higher gain than with resistors for the same DC voltage drop, with a minimum impact in noise figure.

It was also demonstrated that despite the rough approximations made, such as neglecting parasitics, output conductances and distortion generation mechanisms, the equations used for both conversion gain and noise factor were accurate.

Simulation results of a circuit implemented in a 130 nm CMOS technology were presented. For comparison, we also have shown the performance of a conventional mixer with resistors. Both circuits have the same power consumption of 3.6 mW from a 1.2 supply. For the MOSFET-only mixer we achieved a gain of 20 dB (about 6 dB improvement), with NF equal to 9.5 dB.

References

[1] B. Razavi, *RF Microelectronics*. Prentice-Hall, 1998.
[2] T. H. Lee, *The Design of CMOS Radio Frequency Integrated Circuits (2nd edition)*. Cambridge University Press, 2004.
[3] J. Crols and M. Steyaert, *CMOS Wireless Transceiver Design*. Kluwer, 1997.
[4] L. B. Oliveira, J. R. Fernandes, I. M. Filanovsky, C. J. Verhoeven, and M. M. Silva, *Analysis and Design of Quadrature Oscillators*. Springer, 2008.
[5] K. Iniewski, *VLSI Circuits for Biomedical Applications*. Artech House, 2008.
[6] M. T. Terrovitis and R. G. Meyer, "Noise in current-commutating cmos mixers," *IEEE J.Solid-State Circuits*, vol. 34, no. 6, jun 1999.
[7] ——, "Intermodulation distortion in current-commutating cmos mixers," *IEEE J.Solid-State Circuits*, vol. 35, no. 10, pp. 1461–1473, oct 2000.
[8] H. Darabi and A. A. Abidi, "Noise in rf-cmos mixers: A simple physical model," *IEEE Transactions On J.Solid-State Circuits*, vol. 35, no. 1, jan 2000.
[9] I. Bastos, L. B. Oliveira, J. Goes, and M. Silva, "Mosfet-only wideband lna with noise canceling and gain optimization," *Proceedings of the 17th International Conference Mixed Design of Integrated Circuits and Systems (MIXDES)*, pp. 306–311, jun 2010.
[10] T. Tille, J. Sauerbrey, M. Mauthe, and D. Schmitt-Landsiedel, "Design of low-voltage mosfet-only sigma-delta modulators in standard digital cmos technology," *IEEE Trans. Circuits and Systems - I*, vol. 51, no. 1, pp. 96–109, jan 2004.